Journal of Catalysis 276 (2010) 76–84

Contents lists available at ScienceDirect

Journal of Catalysis

journal homepage: www.elsevier.com/locate/jcat

Copper-catalyzed propylene epoxidation by oxygen: Significant promoting effect of vanadium on unsupported copper catalyst

Lüjuan Yang, Jieli He, Qinghong Zhang, Ye Wang *

State Key Laboratory of Physical Chemistry of Solid Surfaces, National Engineering Laboratory for Green Chemical Productions of Alcohols, Ethers and Esters, College of Chemistry and Chemical Engineering, Xiamen University, Xiamen 361005, PR China

ARTICLE INFO

Article history:
Received 12 July 2010
Revised 1 September 2010
Accepted 2 September 2010

Keywords:
Propylene
Epoxidation
Molecular oxygen
Copper catalyst
Vanadium

ABSTRACT

The modification of copper by vanadium significantly enhanced its catalytic performance of propylene epoxidation by oxygen. Synergistic effects existed between copper and vanadium, and the catalysts with V/Cu atomic ratios of 0.11–0.20 exhibited better propylene oxide (PO) formation activity. The dispersion of copper was enhanced by vanadium, and this might contribute to the increase in catalytic activity. The pre-reduction of catalyst resulted in better performances than the oxidative pretreatment, and an induction period was observed for PO formation over the reduced catalyst. In situ XRD measurements revealed that Cu^0 in the reduced catalyst was partially transformed into Cu_2O in propylene oxidation, and the presence of VO_x promoted this transformation. Structure–performance correlations demonstrate that Cu^I accounts for propylene epoxidation. Vanadium species at lower valence states (V^{III} and V^{IV}) may participate in the activation of oxygen. The presence of VO_x also suppressed the reactivity of lattice oxygen in the working catalyst.

1. Introduction

Propylene oxide (PO) is a versatile synthetic intermediate. In the current chemical industry, PO is mainly produced by the chlorohydrin process and the organic hydroperoxide process, but both processes produce large amounts of by-products and are not atomically economic. The development of efficient catalysts that can work for the direct epoxidation of C_3H_6 by a green oxidant has attracted much attention [1,2]. TS-1 was known to be capable of efficiently catalyzing the epoxidation of C_3H_6 by H_2O_2 in liquid phase [3]. However, the comparable market value of H_2O_2 to PO limits the direct use of H_2O_2 for C_3H_6 epoxidation [2]. Many research groups have focused on the in situ production of H_2O_2 from H_2–O_2 gas mixture for C_3H_6 epoxidation [4–10]. The Au/TiO_2- or Au/Ti-containing molecular sieve-based vapor-phase C_3H_6 epoxidation catalysts, which can produce PO with a high selectivity (>90%), have attracted particular research interests [5–10].

The heterogeneously catalyzed epoxidation of C_3H_6 by O_2 without using a sacrificial reductant is the most desirable route for the PO production. However, there has been less success in the development of efficient catalysts for the epoxidation of C_3H_6 using O_2 as a sole oxidant, although the Ag-catalyzed epoxidation of ethylene by O_2 has been commercialized for several decades [1,2]. Much research effort has been paid to the epoxidation of C_3H_6 by O_2 using Ag-based catalysts [1,2,11–20]. PO selectivity could hardly exceed 50% even at low C_3H_6 conversions (<5%) over most catalysts, although a recent study disclosed that the deposition of Ag_3 cluster onto ultrathin alumina film led to a catalyst with higher PO selectivity [20]. Small Au nanoclusters deposited on Al_2O_3, TiO_2, and TS-1 were recently demonstrated to catalyze the epoxidation of C_3H_6 by O_2–H_2O with moderate performances [21–23].

On the other hand, through a series of surface chemistry studies over Ag and Cu single-crystal surfaces pre-covered by adsorbed oxygen species, Lambert and co-workers [24,25] indicated that Cu surfaces was more selective than Ag surfaces for the epoxidation of alkenes with allylic C–H bonds. The lower basicity (nucleophilicity) of oxygen atoms on Cu surfaces was proposed to favor the epoxidation [26]. However, it was also suggested that only isolated oxygen atoms over Cu surfaces could lead to epoxidation, while island of "oxidic" oxygen could not [24]. On the other hand, Monnier and Hartley [27] once pointed out that metallic Cu (Cu^0) may be difficult to function as a true epoxidation catalyst under reaction conditions because it may be readily oxidized into Cu_2O or CuO in the presence of O_2.

A few Cu-based catalysts, including NaCl-modified $VCe_{1-x}Cu_x$ oxide [28], NaCl-modified Cu/SiO_2 [29], and Cu/SiO_2 [30], could work for the epoxidation of C_3H_6 by O_2. The pre-reduction was required, and Cu^0 was proposed as the active site of these catalysts. The main problem of these catalysts is that reasonable PO selectivities (>10%) could only be obtained at very low C_3H_6 conversions (<0.5%). The increase in C_3H_6 conversion to >1% by raising reaction temperature or O_2 partial pressure led to the decrease in PO

* Corresponding author. Fax: +86 592 2183047.
E-mail address: wangye@xmu.edu.cn (Y. Wang).

0021-9517/$ - see front matter © 2010 Elsevier Inc. All rights reserved.
doi:10.1016/j.jcat.2010.09.002

selectivity to <5% [28–30]. The transformation of Cu^0 to oxidized copper species was believed to be detrimental to C_3H_6 epoxidation. On the other hand, we found and reported that, in the presence of modification by alkali metal ion (e.g., K^+), SBA-15- or silica-dispersed $Cu^{II}O_x$ clusters without pre-reduction could catalyze the epoxidation of C_3H_6 by O_2 more efficiently [31–33]. Our studies suggested that Cu^I species generated during the reaction functioned as the active site for C_3H_6 epoxidation by O_2 [33]. Recently, Li and co-workers [34] also demonstrated that highly dispersed Cu species or small CuO_x clusters modified by K^+ were efficient for C_3H_6 epoxidation. Isolated-like ionic Cu^{II} species were recently suggested to be responsible for C_3H_6 epoxidation by O_2 [35]. It is clear that more studies are required to gain further information about the nature of active copper sites responsible for C_3H_6 epoxidation by O_2.

The oxidation of C_3H_6 by O_2 over unsupported copper may provide more direct insights. Recently, we investigated the catalytic behaviors of unsupported copper powder starting from Cu^0 and the modifying effect of various transition metals or metal oxides. We found that the modification of copper by vanadium could significantly enhance both the activity and selectivity for PO formation. It is of interest that neither supports nor conventional promoters such as alkali metal halides are needed for PO formation in the present system. This paper reports the catalytic behaviors and the structural characteristics of the VO_x-modified Cu catalysts. The role of vanadium modification in enhancing PO formation and the nature of active sites are discussed with the aim of providing insights into the requirements for rational design of efficient epoxidation catalysts.

2. Experimental

2.1. Catalyst preparation

Cu catalysts with different modifiers were prepared by a co-precipitation method. Typically, an aqueous solution of Na_2CO_3 (0.06 mol dm^{-3}) was added dropwise to the mixed aqueous solution containing $Cu(NO_3)_2$ (0.05 mol dm^{-3}) and the other transition metal (M) precursor. The ratio of M/Cu in the final catalyst was regulated by the concentration of the precursor containing M. For the preparation of VO_x-modified Cu catalysts, NH_4VO_3 was used as the precursor of vanadium. The precipitate was recovered by filtration, followed by washing thoroughly with deionized water and drying at 373 K overnight. The dried powdery sample was calcined in air at 673 K for 4 h. The single copper catalyst without modification was prepared with the same procedure except for the addition of other transition metal precursors.

2.2. Catalyst characterization

The ratio of the other transition metal to copper in each catalyst was determined by inductively coupled plasma (ICP) optical emission spectrometry using an Agilent ICP-MS 4500–300 after the sample was completely dissolved in an acid medium. The BET surface area was measured by N_2 sorption at 77 K with a Micromeritics Tristar 3000 surface area and porosimetry analyzer.

Powder X-ray diffraction (XRD) patterns were recorded on a Phillips X'Pert Pro Super X-ray diffractometer equipped with X'Celerator detection system and XRK reactor attachment for in situ XRD measurements. Cu Kα radiation (40 kV and 30 mA) was used as the X-ray source. X-ray photoelectron spectroscopy (XPS) was measured with a PHI Quantum 2000 Scanning ESCA Microprobe equipment using monochromatic Al Kα radiation. For each measurement, the sample after pretreatments or catalytic reactions was sealed in a sample tube and was transferred to evacuation chamber instantly to avoid exposure to open air. H_2 and C_3H_6 temperature-programmed reduction (H_2–TPR and C_3H_6–TPR) measurements were performed using a Micromeritics AutoChem 2920 II instrument. Typically, the sample loaded in a quartz reactor was first pretreated with a gas flow containing O_2 and He at 673 K for 0.5 h, followed by purge with high-purity N_2 and cooling down to 313 K. For H_2–TPR, a H_2–Ar gas flow (5 vol.% H_2) was introduced into the reactor, and the temperature was raised to 1073 K at a rate of 10 K min^{-1}. The consumption of H_2 was monitored by a thermal conductivity detector (TCD). For C_3H_6–TPR, a C_3H_6–He (8 vol.% C_3H_6) gas mixture was introduced into the catalyst after pretreatment in O_2-containing gas flow followed by purge with high-purity He for 1 h. Then, the temperature was raised to 773 K at a rate of 10 K min^{-1} and was kept at 773 K for 0.5 h. The products formed during this process were monitored by a mass spectrometer (ThermoStar GSD 301T2). The H_2–TPR and C_3H_6–TPR were also performed for the catalyst after in situ reaction.

The dispersion of Cu was measured by a N_2O titration method [36,37]. Typically, the catalyst after H_2 reduction at 673 K was titrated by N_2O oxidation at room temperature, and it is known that only the surface Cu^0 can be oxidized to Cu^I in this step [36,37]. After this step, H_2–TPR was carried out in a H_2–Ar (5 vol.% H_2) gas flow up to 873 K. Subsequently, the catalyst was oxidized in air at 873 K, and then another H_2–TPR was performed in the H_2-Ar gas flow (5 vol.% H_2) up to 873 K. Assuming that the H_2 consumption in the first H_2–TPR was X_1 and that in the second H_2–TPR was X_2, we could calculate the dispersion of copper (D) by the following equation [36,37],

$$D(\%) = \frac{2X_1}{X_2} \times 100\% \quad (1)$$

2.3. Catalytic reaction

Catalytic reactions were carried out using a fixed-bed quartz reactor operated at atmospheric pressure. Unless otherwise stated, the catalyst was pretreated in the quartz reactor with H_2 gas flow (40 mL min^{-1}) at 673 K for 1 h, followed by purging with high-purity N_2 at the same temperature for 0.5 h before reaction. The reaction was started by introducing a reactant gas flow containing C_3H_6, O_2, and N_2 (for dilution) to the reactor after the catalyst was cooled down to a desired reaction temperature. The products along with the unreacted reactants were analyzed by on-line gas chromatography. All of the lines and valves between the exit of the reactor and the gas chromatographs were heated to 393 K to prevent condensation of the products. The results obtained after 35 min of reaction were typically used for discussion unless otherwise mentioned.

3. Results

3.1. Catalytic performances of various modified Cu catalysts for the epoxidation of C_3H_6 by O_2

Table 1 shows the catalytic performances of various transition metal- or metal oxide-modified copper catalysts. A very low C_3H_6 conversion (0.045%) was obtained over the copper catalyst without any modification at 503 K. The increase in the reaction temperature to 573 K increased C_3H_6 conversion to 0.77%, but PO selectivity decreased from 9.2% to 1.9%. Thus, copper alone was not effective for C_3H_6 epoxidation by O_2. The modification of Cu catalyst with many transition metals or metal oxides increased C_3H_6 conversion, but only the modification with vanadium, molybdenum, or zinc could significantly enhance PO selectivity. Particularly, the modification with vanadium markedly increased both C_3H_6 conversion

Table 1
Catalytic performances of various modified Cu catalysts for C_3H_6 epoxidation by O_2.[a]

Catalyst	M/Cu (molar ratio)	Temperature (K)	Conversion (%)	Selectivity[b] (%)		
				PO	Acrolein	CO_x
Cu	–	503	0.045	9.2	81	6.8
Cu	–	573	0.77	1.9	43	47
TiO_x–Cu	0.038	523	1.1	5.2	11.2	80
VO_x–Cu	0.047	503	2.5	14	9.6	74
VO_x–Cu	0.11	503	2.7	16	11	70
CrO_x–Cu	0.056	503	1.2	2.5	23	73
MnO_x–Cu	0.054	525	1.8	1.9	26	70
FeO_x–Cu	0.063	503	0.18	5.1	68	24
CoO_x–Cu	0.051	503	0.58	2.7	31	65
NiO_x–Cu	0.050	503	0.44	2.0	28	68
ZnO_x–Cu	0.053	598	0.36	18	47	33
MoO_x–Cu	0.048	503	0.53	16	5.4	62
MoO_x–Cu	0.083	503	0.59	13	5.6	64
WO_x–Cu	0.045	503	1.95	1.2	15	81
Ag–Cu	0.022	551	0.92	0.51	33	64
Au–Cu	0.012	519	1.1	1.3	28	69

[a] Reaction conditions: $W = 0.20$ g; $P(C_3H_6) = 8.0$ kPa, $P(O_2) = 4.0$ kPa; $F(\text{total}) = 50$ mL min^{-1}.
[b] Other products include propanol, acetone, allyl alcohol, and acetaldehyde.

and PO selectivity. A moderate selectivity (16%) could be obtained at a reasonably high C_3H_6 conversion (2.7%) over the VO_x-modified Cu catalyst. This combination of C_3H_6 conversion and PO selectivity is superior to those obtained over other Cu-based catalysts starting from Cu^0, where the increase in C_3H_6 conversions to >1% dramatically decreased PO selectivity to <10% [28–30]. Only the K^+-modified CuO_x/SBA-15 or CuO_x/SiO_2 catalysts starting from Cu^{2+} exhibited better catalytic performances [31–34]. Thus, we focused our detailed studies on the VO_x-modified Cu catalytic system.

3.2. Effect of V/Cu ratio on catalytic performances of the VO_x-modified Cu catalysts

Table 2 shows the effect of the V/Cu ratio on catalytic performances of the VO_x-modified Cu catalysts. Both single copper and single vanadium catalysts only provided very low C_3H_6 conversions under the reaction conditions in Table 2. Moreover, no PO was formed over the single vanadium catalyst. In addition to acrolein, *i*-propanol was also formed as a main partial oxidation product over the single vanadium catalyst. The combination of VO_x with Cu not only markedly increased C_3H_6 conversions but also significantly enhanced PO selectivity. Thus, there exists a synergistic effect between vanadium and copper for PO formation. The catalysts with V/Cu ratios of 0.11 and 0.20 exhibited almost the same PO selectivity and PO formation rate, which were better than those with other V/Cu ratios. For the catalyst with a higher V/Cu ratio (0.29), PO selectivity became significantly lower.

3.3. Catalytic behaviors of VO_x-modified Cu catalysts under different reaction conditions

Fig. 1 shows the catalytic behaviors of the VO_x–Cu catalyst with a V/Cu ratio of 0.11 along with the single Cu catalyst as a function of reaction temperature. C_3H_6 conversions increased exponentially with reaction temperature over both catalysts. Good straight lines were obtained for both catalysts when the logarithm of the rate of C_3H_6 conversion was plotted against the reciprocal of temperature (Supplementary material, Fig. S1). The apparent activation energy values calculated were 109 and 78 kJ mol^{-1} for Cu and VO_x–Cu (V/Cu = 0.11) catalysts, respectively. The decrease in the apparent activation energy after VO_x modification may imply the change in the reaction route.

Over Cu catalyst, acrolein was the dominant partial oxidation product, and PO was also formed at lower temperatures with a maximum selectivity of ~10%, where C_3H_6 conversion was less than 0.2% (Fig. 1A). The increase in temperature decreased the selectivities to both acrolein and PO; PO selectivity became less than 2% at a C_3H_6 conversion of 0.77%. After the modification of Cu by VO_x (V/Cu = 0.11), PO became a main partial oxidation product (Fig. 1B). PO selectivity of 16% could be sustained at a C_3H_6 conversion of 2.7%.

The change of catalytic performances with the contact time, which is expressed by the ratio of catalyst weight to total flow rate (W/F), is shown in Fig. 2. Different temperatures were adopted for Cu (Fig. 2A, 593 K) and VO_x–Cu (V/Cu = 0.11) (Fig. 2B, 503 K)

Table 2
Effect of V/Cu ratio on catalytic performances of VO_x-modified Cu catalysts for C_3H_6 epoxidation by O_2.[a]

V/Cu (molar ratio)	Conversion (%)	Selectivity[b] (%)			PO formation rate (mmol g^{-1} h^{-1})
		PO	Acrolein	CO_x	
0	0.045	9.2	81	6.8	0.0022
0.048	2.5	14	9.6	74	0.18
0.11	2.7	16	11	70	0.23
0.20	2.7	16	7.2	73	0.23
0.29	2.0	4.5	5.8	83	0.048
∞[c]	0.18	0	6.8	74	0

[a] Reaction conditions: $W = 0.20$ g; $T = 503$ K; $P(C_3H_6) = 8.0$ kPa, $P(O_2) = 4.0$ kPa; $F(\text{total}) = 50$ mL min^{-1}.
[b] Other products include propanol, acetone, allyl alcohol, and acetaldehyde.
[c] Single V_2O_5 was used as the precursor of catalyst, and *i*-propanol was also formed as a main partial oxidation product along with acrolein and CO_x.

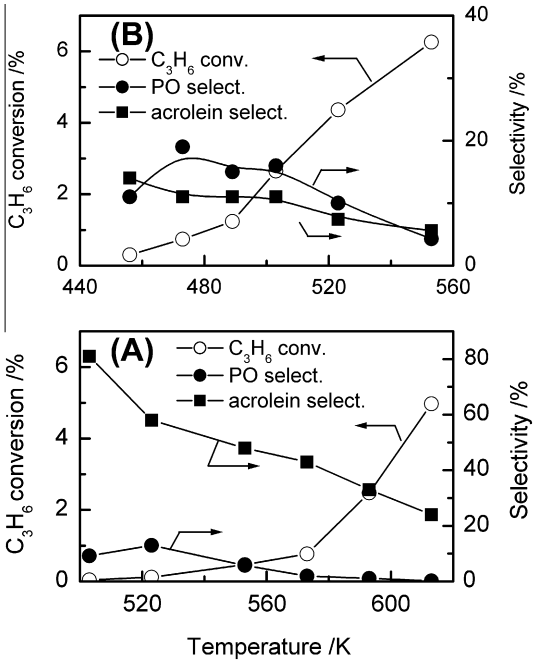

Fig. 1. Catalytic behaviors of the single Cu (A) and the VO_x–Cu (V/Cu = 0.11) (B) catalysts for the oxidation of C_3H_6 by O_2 at different temperatures. Reaction conditions: W = 0.20 g; $P(C_3H_6)$ = 8.0 kPa; $P(O_2)$ = 4.0 kPa; F(total) = 50 mL min^{-1}.

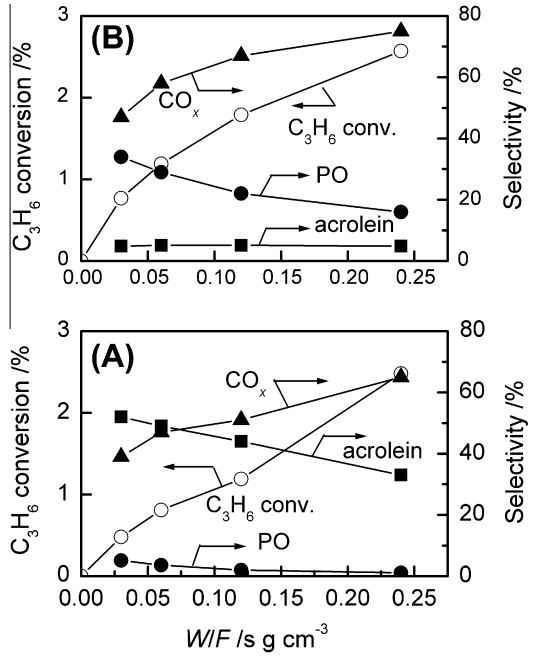

Fig. 2. Effect of contact time (W/F) on catalytic behaviors of the single Cu (A) and the VO_x–Cu (V/Cu = 0.11) (B) catalysts for the oxidation of C_3H_6 by O_2. Reaction conditions: $P(C_3H_6)$ = 8.0 kPa; $P(O_2)$ = 4.0 kPa; T = 593 K (A); T = 503 K (B).

catalysts to obtain comparable C_3H_6 conversions. Fig. 2 further demonstrates that the main partial oxidation product is changed from acrolein to PO after the modification of Cu by VO_x. The increase in contact time decreased the selectivity to acrolein or PO and increased that to CO_x, indicating that CO_x was partially produced through the over-oxidation of acrolein or PO. Since CO_x was also formed even at very short contact times (very low C_3H_6 conversions), a part of CO_x might be formed in parallel to acrolein or PO

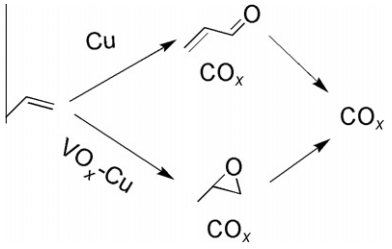

Fig. 3. Main reaction routes for the oxidation of C_3H_6 by O_2 over the single Cu and the VO_x–Cu catalysts.

as primary products. The main reaction routes over Cu and VO_x–Cu (V/Cu = 0.11) catalysts are summarized in Fig. 3.

3.4. Effect of pretreatment on catalytic behaviors of the VO_x–Cu catalyst

As described previously, Cu^0 was proposed for C_3H_6 epoxidation by O_2 over several Cu-based catalysts, and the pre-reduction of these catalysts was necessary [28–30]. On the other hand, our previous work with the K^+-modified CuO_x/SBA-15 or CuO_x/SiO_2 showed that the oxidatively pretreated catalyst could afford superior catalytic performances for PO formation [31–33], and the Cu^I generated during the reaction was demonstrated to be responsible for C_3H_6 epoxidation [33]. To gain insights into the nature of the active site for the VO_x-modified Cu catalyst, we investigated the effect of pretreatment on catalytic performances.

The catalytic performances of the VO_x–Cu (V/Cu = 0.11) catalyst pretreated by air and by H_2 are compared in Fig. 4. For the catalyst after pretreatment by air (F = 40 mL min^{-1}) at 673 K, followed by purging with high-purity N_2, the steady state was quickly achieved without induction period (Fig. 4A). C_3H_6 conversion was stable at ~0.6% after 15 min of reaction, and the selectivities to acrolein and PO were ~27% and ~4%, respectively, at 503 K. On the other hand, the pre-reduction by H_2 at 673 K cause the appearance of an obvious induction period (Fig. 4B). The catalyst was almost inactive at the very initial stage, and C_3H_6 conversion increased significantly with time on stream. At a time on stream of 35 min, C_3H_6 conversion increased to 2.6%, significantly higher than the steady-state C_3H_6 conversion over the catalyst pretreated by air. PO selectivity also increased significantly from ~3% to ~16% in the initial 35 min. Further prolonging of the time on stream slightly decreased C_3H_6 conversion, but PO selectivity kept almost unchanged.

3.5. Structural characteristics of the VO_x-modified Cu catalysts

3.5.1. Surface area and Cu dispersion

The BET surface areas derived from N_2-physisorption and the dispersion of copper evaluated from the N_2O titration method for the VO_x–Cu catalysts after reduction are listed in Table 3. The addition of small amount of vanadium into copper increased the BET

Table 3
BET surface areas and Cu dispersions for the VO_x-modified Cu catalysts.

Catalyst	BET surface area (m^2 g^{-1})	Cu dispersion (%)
Cu	2.9	0.48
VO_x–Cu (V/Cu = 0.047)	4.7	2.2
VO_x–Cu (V/Cu = 0.11)	11	2.6
VO_x–Cu (V/Cu = 0.20)	9.5	4.0
VO_x–Cu (V/Cu = 0.29)	24	4.7

surface area and the dispersion of Cu. This implies that there may exist strong interactions between copper and vanadium species in the VO_x–Cu catalysts.

3.5.2. Crystalline structure

In situ XRD measurements were performed to gain information on the crystalline structures of the VO_x-modified Cu catalysts. The sample was pressed in an alumina sample holder, which was set in the in situ XRK chamber. Fig. 5 shows the XRD patterns of the calcined VO_x–Cu samples with V/Cu ratios of 0, 0.11, and 0.29 before H_2 reduction. The main diffraction peaks of these samples could be ascribed to monoclinic CuO. For the sample with a higher vanadium content (V/Cu = 0.29), very weak peaks attributable to $Cu_5V_2O_{10}$ crystallites at 2θ of ~29.8° and ~43.0° could be discerned in the enlarged curve (10 times enlarged, curve c in Fig. 5B). This observation further suggests the strong interaction between copper and vanadium species.

After the reduction by H_2 at 673 K for 1 h, three main diffraction peaks at 2θ of 43.8°, 50.8°, and 74.4° were observed for the single Cu sample (Fig. 6), which were assignable to (1 1 1), (2 0 0), and (3 1 1) reflections of cubic metallic copper. For the VO_x–Cu samples, the peaks ascribed to metallic Cu shifted to lower diffraction angles, i.e., 43.2°, 50.2°, and 73.9°, suggesting that the lattice of metallic Cu was slightly expanded in the presence of vanadium species. Moreover, besides the three main diffraction lines of metallic Cu, weak peaks at 2θ of 24.3°, 33.0°, 36.1°, and 53.8°, which could be ascribed to the crystalline phase of V_2O_3, were also observed in the enlarged curves (Fig. 6B). Thus, after H_2 reduction at 673 K, the VO_x–Cu catalysts mainly contain cubic metallic Cu along with small amounts of V_2O_3 crystallites.

Figs. 7 and 8 show the changes of XRD patterns with reaction time in a gas flow containing C_3H_6 and O_2 [$P(C_3H_6)$ = 8 kPa, $P(O_2)$ = 4 kPa] under reaction conditions shown in Table 2. The time of zero denotes the point just before the introduction of reactant gas, and both the single Cu and the VO_x–Cu catalysts contain metallic Cu as the sole Cu-related phase. For the single Cu catalyst (Fig. 7), the cubic metallic Cu remained as the main crystalline phase after 272 min of reaction. Weaker diffraction peaks at 2θ of 36.8° and 61.8° also appeared after 48 min of reaction. These peaks could be assigned to the (1 1 1) and (2 2 0) reflections of cubic Cu_2O phase. On the other hand, for the VO_x–Cu (V/Cu = 0.11) catalyst, diffraction peaks belonging to metallic Cu decreased markedly after the introduction of reactant gas, and the diffraction peaks at 2θ of 36.8° and 61.6°, ascribed to cubic Cu_2O, became stronger after 48 min of reaction (Fig. 8). In addition to these peaks, weak

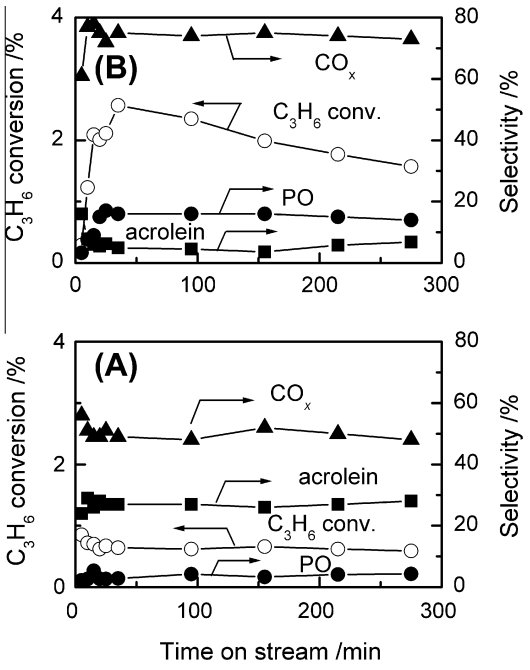

Fig. 4. Changes of catalytic performances with time on stream for the oxidation of C_3H_6 over the VO_x–Cu (V/Cu = 0.11) catalyst after different pretreatments. (A) Pretreated by air, (B) pretreated by H_2. Reaction conditions: W = 0.20 g; $P(C_3H_6)$ = 8.0 kPa; $P(O_2)$ = 4.0 kPa; F(total) = 50 mL min^{-1}; T = 503 K.

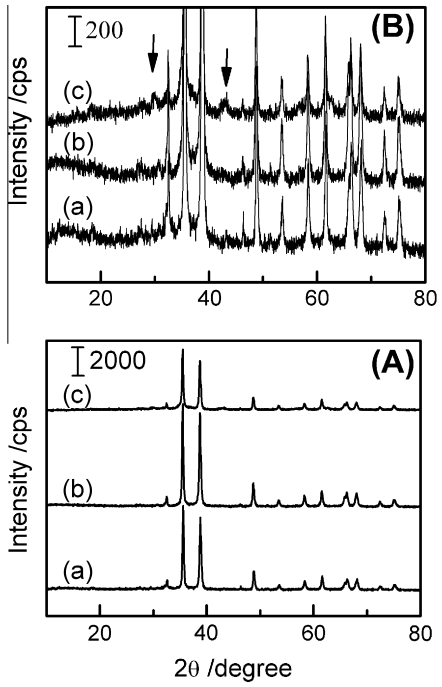

Fig. 5. XRD patterns for the calcined catalysts. (a) CuO, (b) VO_x–CuO (V/Cu = 0.11), (c) VO_x–CuO (V/Cu = 0.29).

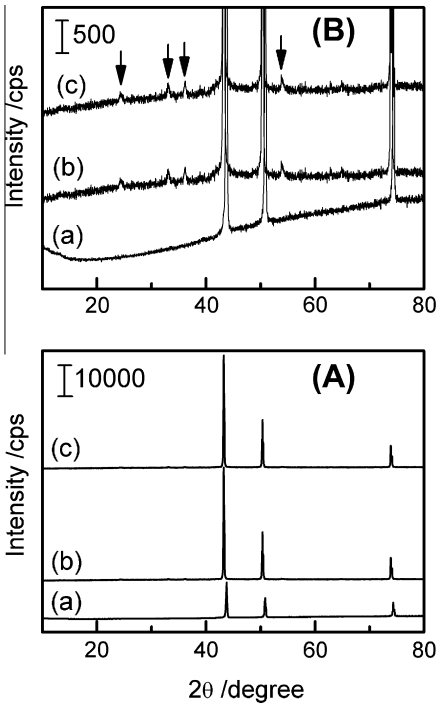

Fig. 6. XRD patterns for the H_2-reduced catalysts. (a) Cu, (b) VO_x–Cu (V/Cu = 0.11), (c) VO_x–Cu (V/Cu = 0.29).

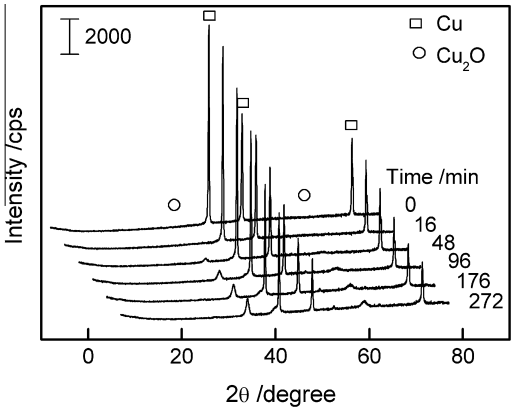

Fig. 7. In situ XRD patterns for the H_2-reduced Cu catalyst in reactant gas flow. Reaction conditions: $P(C_3H_6)$ = 8.0 kPa; $P(O_2)$ = 4.0 kPa; F(total) = 50 mL min^{-1}; T = 503 K.

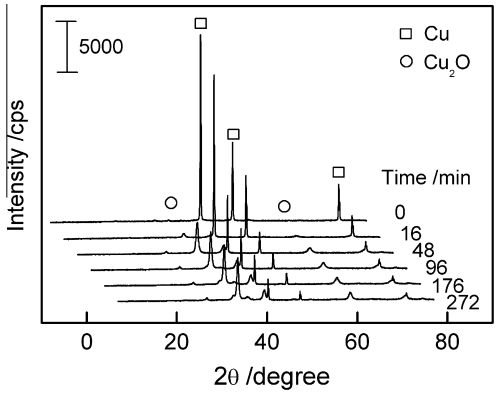

Fig. 8. In situ XRD patterns for the H_2-reduced VO_x–Cu (V/Cu = 0.11) catalyst in reactant gas flow. Reaction conditions: $P(C_3H_6)$ = 8.0 kPa; $P(O_2)$ = 4.0 kPa; F(total) = 50 mL min^{-1}; T = 503 K.

diffraction peaks at 2θ of 29.7° and 42.4°, attributable to the (1 1 0) and (2 0 0) of cubic Cu_2O, were also observed. In other words, the cubic Cu_2O became the main phase in the working VO_x–Cu catalyst. Thus, the modification by vanadium accelerated the transformation of metallic Cu into Cu_2O in the reactant gas flow. No XRD peaks ascribed to vanadium-related compounds were detectable for the VO_x–Cu catalyst during reaction.

We also investigated the change of XRD patterns with reaction time in the reactant gas flow for the VO_x–Cu (V/Cu = 0.11) catalyst after air pretreatment. No significant changes in XRD patterns were observed during reaction. After 272 min of reaction under the same conditions using in Figs. 7 and 8, CuO remained as the main phase.

3.5.3. Oxidation states of surface copper and vanadium species

To gain information about the oxidation states of copper and vanadium on catalyst surface of the working catalyst, we further performed XPS studies for the VO_x–Cu catalyst immediately after the epoxidation reaction at 503 K. As shown in Fig. 9, the binding energy values of Cu 2p3/2 were observed at 932.2 and 932.5 eV for the single Cu and the VO_x–Cu (V/Cu = 0.11) catalysts, respectively. These binding energy values can be attributed to either Cu^0 or Cu^I because these two oxidation states show similar Cu 2p XPS spectra [38]. Cu L_3VV Auger lines are generally used to discriminate these two oxidation states, and it is known that the L_3VV Auger line of Cu^I lies at lower electron kinetic energy than that of Cu^0 [38]. As shown in Fig. 9B, the Cu L_3VV Auger peak for

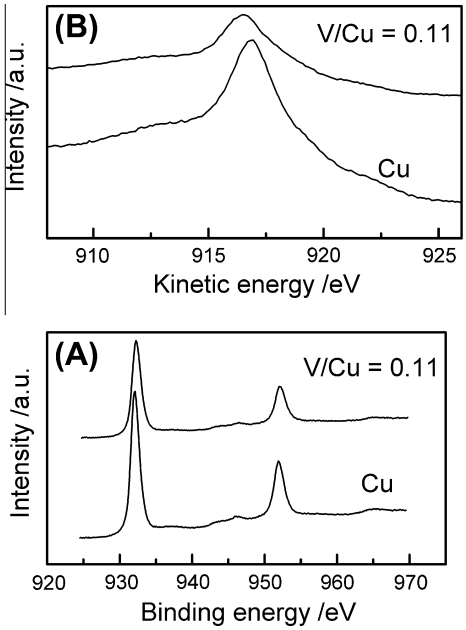

Fig. 9. Cu 2p XPS (A) and Cu L_3VV AES (B) spectra for the Cu and VO_x–Cu (V/Cu = 0.11) catalysts immediately after the epoxidation reactions. Reaction conditions: $P(C_3H_6)$ = 8.0 kPa; $P(O_2)$ = 4.0 kPa; F(total) = 50 mL min^{-1}; T = 503 K.

the catalyst with VO_x modification shifted to lower kinetic energy position centered at ~916.5 eV, corresponding to Cu^I [38]. This observation confirms that the copper species on the surface of the VO_x–Cu catalyst is mainly in Cu^I state during the epoxidation reaction.

Fig. 10 shows the V 2p spectra for the VO_x–Cu (V/Cu = 0.11) samples before and after H_2 reduction and after C_3H_6 epoxidation. Before H_2 reduction, the binding energy of V 2p3/2 was located at 517.5 eV, assignable to that of V^V [39]. The binding energy of V 2p3/2 shifted to 515.8 eV after H_2 reduction, which could be attributed to that of V^{III} [39]. This result is consistent with the XRD result that V_2O_3 phase was observed after H_2 reduction (Fig. 6). After the epoxidation reaction, the binding energy of V 2p3/2 shifted to a slightly higher value (516.2 eV). This observation suggests the occurrence of the re-oxidation of V^{III} to V^{IV} during reaction [39]. We also estimated the surface V/Cu ratios from XPS measurements for the VO_x–Cu (V/Cu = 0.11 and 0.29) catalysts, and the values

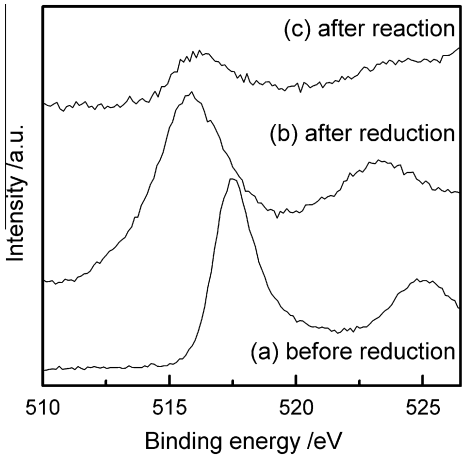

Fig. 10. V 2p XPS spectra for the VO_x–Cu (V/Cu = 0.11) catalyst. (a) Before H_2 reduction, (b) after H_2 reduction at 673 K, (c) after reaction under the following conditions: $P(C_3H_6)$ = 8.0 kPa; $P(O_2)$ = 4.0 kPa; F(total) = 50 mL min^{-1}; T = 503 K.

were 0.30 and 0.57, respectively, indicating that some VO_x species were segregated on catalyst surfaces.

We performed diffuse reflectance UV–vis spectroscopic studies for the VO_x–Cu (V/Cu = 0.11) samples before and after H_2 reduction and after C_3H_6 epoxidation to gain further information about the chemical states of vanadium species. The results also suggested that the vanadium species were reduced from V^V to V^{III} after H_2 reduction, and some of the V^{III} species were oxidized to V^{IV} after C_3H_6 epoxidation at 503 K (Supplementary material, Fig. S2).

3.6. Reducibility and reactivity of lattice oxygen

3.6.1. H_2–TPR

H_2–TPR profiles for the VO_x–Cu catalysts together with the single Cu and V_2O_5 after calcination are shown in Fig. 11A. Our single Cu catalyst after calcination showed a main reduction peak at 545 K together with a shoulder peak at 583 K, and these peaks should correspond to the reduction of CuO to Cu^0. Single V_2O_5 exhibited reduction peaks at 941 and 973 K, which may be contributed by the reduction of V^V to V^{IV} and V^{IV} to V^{III}. The reduction of the VO_x–Cu (V/Cu = 0.11 and 0.29) catalysts after calcination occurred in the range of 450–700 K with a main peak at ~650 K and shoulder peaks at lower temperatures. Our quantitative calculations suggested that these reduction peaks could not be only ascribed to the reduction of Cu^{II} to Cu^0 and should involve the reductions of both copper and vanadium. By assuming that a part of H_2 was consumed for the reduction of Cu^{II} to Cu^0, we estimated that the change in oxidation state of vanadium after H_2 reduction was 1.8 for the VO_x–Cu (V/Cu = 0.11) sample, roughly corresponding to the reduction V^V to V^{III}. This is consistent with the XRD and XPS measurements described above (Figs. 6 and 10). H_2–TPR profiles in Fig. 11A also informed us that the reduction of vanadium species was significantly promoted by copper, and this also implied that strong interactions existed between vanadium and copper species in our catalysts. It is likely that H_2 is dissociatively chemisorbed on the reduced copper surface and the H atoms subsequently spillover to the neighboring VO_x species to enhance its reduction.

We further performed H_2–TPR for the catalyst immediately after the catalytic reaction in ($C_3H_6 + O_2$) flow at 503 K for 35 min, followed by purging with He and cooling down to 303 K. The catalyst was pre-reduced by H_2 at 673 K before the reaction. The single Cu exhibited a reduction peak at 551 K (Fig. 11B). From the in situ XRD result, it is reasonable to speculate that this peak corresponds to the reduction of Cu_2O generated during the reaction to Cu^0. For the catalysts with V/Cu ratios of 0.11 and 0.29, reduction peaks appeared at 668 and 653 K, respectively. These observations suggest that the reactivity of lattice oxygen of Cu_2O in the working catalyst becomes lower after the modification by VO_x species.

3.6.2. C_3H_6–TPR

The reactivity of lattice oxygen with C_3H_6 was investigated using C_3H_6–TPR. Fig. 12 shows the products formed during the C_3H_6–TPR over the single Cu and the VO_x–Cu (V/Cu = 0.11) catalysts after calcination followed by He purge. The reaction of C_3H_6 with the lattice oxygen of the single Cu (CuO) catalyst showed a sharp peak at ~601 K and provided CO_2 as the predominant product together with small fractions of CO and acrolein. The modification of Cu by VO_x (V/Cu = 0.11) changed the C_3H_6–TPR profile significantly. Two broad peaks at 635 and 729 K were observed for CO_2 formation. Besides CO_2, CO and acrolein were also formed with relatively larger fractions over the VO_x–Cu catalyst, and the formations of CO and acrolein also exhibited two broad peaks. These observations allow us to speculate that the reaction of C_3H_6 with the lattice oxygen of CuO produced mainly CO_2 at ~601 K, and this reaction proceeds quickly to completion due to the reduction of Cu^{II} to Cu^0. On the other hand, the reduction of VO_x–Cu catalyst after calcination may proceed in two steps, i.e., Cu^{II} to Cu^I and Cu^I to Cu^0, providing acrolein, CO, and CO_2.

C_3H_6–TPR profiles for the single Cu and the VO_x–Cu catalysts immediately after the catalytic reaction in ($C_3H_6 + O_2$) flow at 503 K for 35 min, followed by purging with He and cooling down to 303 K, are shown in Fig. 13. CO_2 was still the predominant product for the single Cu catalyst, and the reduction occurred at

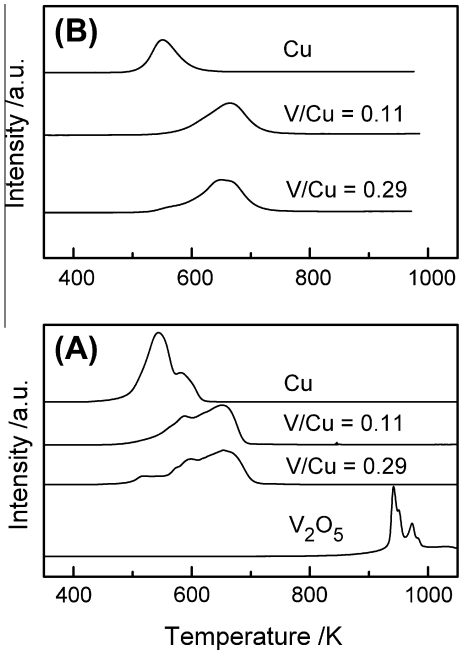

Fig. 11. H_2–TPR profiles for the VO_x–Cu (V/Cu = 0.11 and 0.29) and the single Cu and VO_x catalysts. (A) After calcination, (B) after catalytic reaction under the following conditions: $P(C_3H_6)$ = 8.0 kPa; $P(O_2)$ = 4.0 kPa; F(total) = 50 mL min^{-1}; T = 503 K (catalysts were reduced by H_2 at 673 K before reaction).

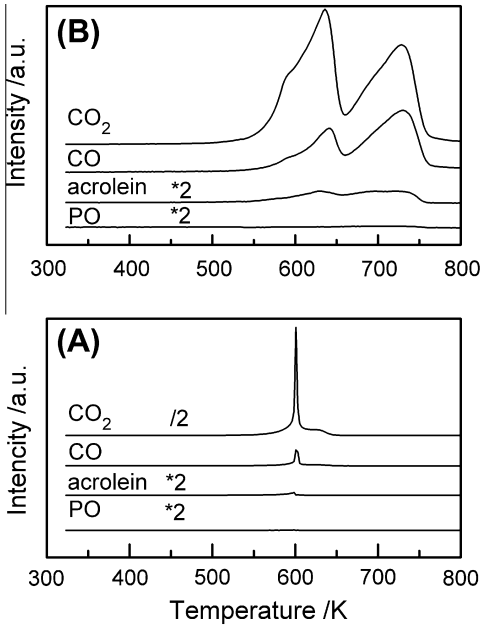

Fig. 12. C_3H_6–TPR profiles for the single Cu (A) and the VO_x–Cu (V/Cu = 0.11) (B) catalysts after calcination.

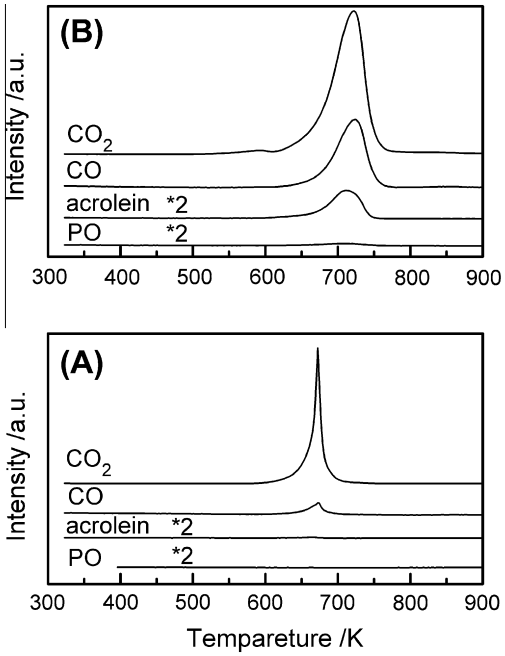

Fig. 13. C_3H_6–TPR profiles for the single Cu (A) and the VO_x–Cu (V/Cu = 0.11) (B) catalysts after catalytic reactions under the following conditions: $P(C_3H_6)$ = 8.0 kPa; $P(O_2)$ = 4.0 kPa; F(total) = 50 mL min^{-1}; T = 503 K (catalysts were reduced by H_2 at 673 K before reaction).

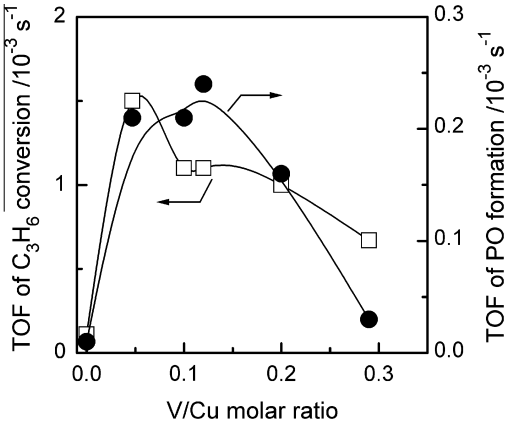

Fig. 14. TOFs for C_3H_6 conversion and PO formation at 503 K over the VO_x–Cu catalysts with different V/Cu ratios.

~672 K, higher than that for the single Cu catalyst after calcination. This indicates that the reactivity of lattice oxygen in Cu_2O is lower than that in CuO. It is of interest that only one broad reduction peak appears for the VO_x–Cu catalyst after reaction. The peak temperatures for the formations of CO_2, CO, and acrolein were 721, 724, and 715 K, respectively. These temperatures were close to those of the second reduction peaks observed for the VO_x–Cu catalyst after calcination (Fig. 12). This further supports our speculation that the VO_x–Cu catalyst after calcination undergoes a two-step reduction (i.e., $Cu^{II} \rightarrow Cu^{I}$ and $Cu^{I} \rightarrow Cu^{0}$) in C_3H_6. Thus, Cu^{I} may be stabilized by the modification with vanadium. The significant shift of reduction peaks to higher temperatures in the presence of VO_x modification (Fig. 13B) indicates that VO_x suppresses the reactivity of lattice oxygen in the working catalyst (associated mainly with Cu_2O).

4. Discussion

Our catalytic measurements showed that copper alone only exhibited a very low PO formation activity, whereas vanadium oxide alone did not catalyze PO formation. The modification of copper by vanadium with a proper V/Cu ratio (0.11–0.20) significantly enhanced the PO formation. Both C_3H_6 conversion and PO selectivity were remarkably promoted by the presence of vanadium modification. PO selectivities of 35% and 16% could be obtained at C_3H_6 conversions of 0.78% and 2.7%, respectively, over the catalyst with a V/Cu ratio of 0.11. These results are still too low to meet the industrial requirement, but the present study on modifying effects of vanadium has provided insights into the active Cu sites for C_3H_6 epoxidation. As mentioned previously, some Cu-based catalysts have shown promising performances for the epoxidation of C_3H_6 by O_2 [28–35]. However, alkali metal ion and/or halide promoters are typically required for obtaining better PO selectivity [28,29,31–34]. Vaughan et al. [30] showed that Cu^0 nanoparticles finely dispersed on silica catalyzed the epoxidation of C_3H_6 by O_2. The present paper has demonstrated for the first time that copper catalysts without alkali metal ion or halide modification and without support can also catalyze C_3H_6 epoxidation by O_2. We have shown that the modification of Cu powder by vanadium is effective for C_3H_6 epoxidation.

We clarified that the dispersion of copper was enhanced by the modification with vanadium (Table 3). To elucidate whether the increase in Cu dispersion is the sole effect of vanadium modification, we have calculated the turnover frequency (TOF) values for C_3H_6 conversion and PO formation at 503 K based on Cu atoms on catalyst surface, i.e., moles of C_3H_6 converted and PO formed per mole of surface Cu per second. As shown in Fig. 14, the TOF values for both C_3H_6 conversion and PO formation are markedly higher over the VO_x–Cu catalysts (V/Cu = 0.048–0.20) than those over the single Cu catalyst. When compared to that over the single Cu catalyst, the TOF for PO formation over the catalyst with a V/Cu ratio of 0.11 increased for more than one order of magnitude. Thus, besides the enhanced Cu dispersion, VO_x may play other important roles in promoting the catalytic performance of Cu catalyst.

The catalyst with a higher V/Cu ratio (0.29) showed significantly lower PO selectivity (Table 2) and lower PO formation activity (Fig. 14), despite its higher Cu surface area. This suggests the importance of a proper ratio of V/Cu for PO formation. We speculate that the extra VO_x species in the catalyst might play negative roles in PO selectivity. One possible negative role of the extra VO_x species may be their acidity. Our NH_3–TPD studies for the catalysts after reactions revealed that the modification of Cu by VO_x resulted in the generation of acidic sites (Supplementary material, Fig. S3). It is known that even weak Lewis acidic sites can catalyze the isomerization of PO to allyl alcohol, which can be readily oxidized to acrolein and CO_x under oxidized conditions [33].

The chemical state of copper should be a key factor in determining the catalytic performances. Several previous studies on Cu-based catalysts proposed that Cu^0 was the active phase for C_3H_6 epoxidation by O_2 [28–30]. On the other hand, we indicated that Cu^{I} was responsible for C_3H_6 epoxidation by O_2 over a K^+-modified CuO_x–SiO_2 catalyst without reduction pretreatment [33]. Su et al. recently argued that both Cu^{I} and Cu^0 were responsible for C_3H_6 epoxidation [34], whereas Onal et al. suggested that the isolated Cu^{2+} might be the active site [35]. Our present study using VO_x-modified Cu catalyst showed that, without H_2 pre-reduction, only very low C_3H_6 conversion and PO selectivity were obtained (Fig. 4A). This suggests that Cu^{II} cannot be the active species for C_3H_6 epoxidation in our system. The pre-reduction is necessary for obtaining high PO formation activity over the present unsupported catalyst. We observed induction periods for both C_3H_6 conversion and PO selectivity over the H_2-reduced VO_x–Cu catalyst (Fig. 4B). The gradual change of Cu^0 to Cu_2O phase was observed

from in situ XRD measurements (Fig. 8). This observation together with the XPS characterization for the sample after reaction suggests that it is not the Cu^0 but the Cu^I that functions for the epoxidation of C_3H_6 by O_2. Our in situ XRD studies further suggest that the presence of VO_x species accelerates the transformation of Cu^0 to Cu^I in reactant gas flow at reaction temperature (Figs. 7 and 8). We speculate that the V_2O_3 species in the H_2-reduced catalyst may easily activate O_2 and the activated oxygen species may then be incorporated into Cu to form Cu_2O.

It is expected that the nature of the active oxygen species determines the reaction route. Generally, the lattice oxygen is nucleophilic and mainly catalyzes the allylic oxidation of C_3H_6 to acrolein. Our previous studies showed that the addition of K^+ into SBA-15 or SiO_2-supported CuO_x shifted the H_2–TPR peak for Cu^{II} to Cu^0 to higher temperatures [31–33]. In the present paper, through H_2–TPR and C_3H_6–TPR for the catalysts after reactions (Figs. 11B and 13), we have demonstrated that the reactivity of lattice oxygen in the working catalyst was suppressed by the presence of VO_x species. Moreover, we have confirmed that the reaction of C_3H_6 with the lattice oxygen in the working catalyst provided acrolein, CO and CO_2, and no formation of PO was observed. This further supports the idea that the lattice oxygen is not responsible for C_3H_6 epoxidation. This may partly explain the experimental fact that the modification of Cu by VO_x shifts the main partial oxidation product from acrolein to PO. Actually, Cu_2O is a well-known catalyst for the allyllic oxidation of C_3H_6 to acrolein [40–42]. Considering that the TOFs for both C_3H_6 conversion and PO formation were remarkably enhanced by VO_x modification, we speculate that active oxygen species with an electrophilic character may be generated over the VO_x–Cu catalyst. Vanadium species at lower valence states (V^{III} and V^{IV}) may play a role in the activation of O_2 to form electrophilic oxygen species. Future studies are needed to elucidate the nature of the active oxygen species over our VO_x–Cu catalysts.

5. Conclusions

The unsupported copper powder was less effective for C_3H_6 epoxidation by O_2. The modification of unsupported copper by vanadium significantly enhanced both C_3H_6 conversion and PO selectivity. The catalyst with a V/Cu atomic ratio of 0.11–0.20 was the most efficient for PO formation. Over the catalyst with a V/Cu ratio of 0.11, PO selectivities of 35% and 16% could be obtained at C_3H_6 conversions of 0.78% and 2.7%, respectively. On the other hand, over the Cu catalyst without modification, higher temperatures (573–593 K) were required for obtaining similar C_3H_6 conversions, and acrolein was the main partial oxidation product. The pretreatment of the VO_x–Cu catalyst was also crucial. The pre-reduction of catalyst by H_2 could lead to significantly better catalytic performances for PO formation than the oxidative pretreatment. We observed an induction period for PO formation over the reduced catalyst. Our characterizations showed that the presence of vanadium caused an increase in the dispersion of copper, which might contribute to the rise in catalytic activity. In situ XRD studies demonstrated that Cu^0 in the reduced catalyst was partially transformed into Cu_2O in propylene oxidation and the existence of VO_x promoted this transformation. XPS studies confirmed that Cu^I mainly existed on the surface of the catalyst after reaction. XPS studies also informed us that some vanadium species were changed from V^{III} to V^{IV} during the reaction. The combination of the characterization results with the catalytic reaction results suggests that Cu^I is the active site for propylene epoxidation and vanadium species at lower valence states (V^{III} and V^{IV}) may play a role in the activation of O_2. Our H_2–TPR and C_3H_6–TPR studies indicated that the presence of vanadium species suppressed the reactivity of lattice oxygen in the working catalyst.

Acknowledgments

This work was supported by the National Natural Science Foundation of China (Nos. 20773099, 20625310 and 20923004), the National Basic Research Program of China (No. 2010CB732303), the Research Fund for the Doctoral Program of High Education (No. 20090121110007), and the Key Scientific Project of Fujian Province (No. 2009HZ0002-1).

Appendix A. Supplementary data

Supplementary data associated with this article can be found, in the online version, at doi:10.1016/j.jcat.2010.09.002.

References

[1] J.R. Monnier, Appl. Catal. A 221 (2001) 73.
[2] T.A. Nijhuis, M. Makkee, J.A. Moulijn, B.M. Weckhuysen, Ind. Eng. Chem. Res. 45 (2006) 3447.
[3] M.G. Clerici, G. Bellussi, U. Romano, J. Catal. 129 (1991) 159.
[4] R. Meiers, U. Dingerdissen, W.F. Hölderich, J. Catal. 176 (1998) 376.
[5] T. Hayashi, K. Tanaka, M. Haruta, J. Catal. 178 (1998) 566.
[6] E.E. Stangland, K.B. Stavens, R.P. Andres, W.N. Delgass, J. Catal. 191 (2000) 332.
[7] A.K. Sinha, S. Seelan, S. Tsubota, M. Haruta, Angew. Chem. Int. Ed. 43 (2004) 1546.
[8] T.A. Nijhuis, T. Visser, B.M. Weckhuysen, Angew. Chem. Int. Ed. 44 (2005) 1115.
[9] B. Chowdhury, J.J. Bravo-Sárez, M. Daté, S. Tsubota, M. Haruta, Angew. Chem. Int. Ed. 45 (2006) 412.
[10] E. Sacaliu, A.M. Beale, B.M. Weckhuysen, T.A. Nijhuis, J. Catal. 248 (2007) 235.
[11] G.Z. Lu, X.B. Zuo, Catal. Lett. 58 (1999) 67.
[12] J. Lu, M. Luo, H. Lei, C. Li, Appl. Catal. A 237 (2002) 11.
[13] A. Palermo, A. Husain, M. Tikhov, R.M. Lambert, J. Catal. 207 (2002) 331.
[14] F. Zemicheael, A. Palermo, M. Tikhov, R.M. Lambert, Catal. Lett. 80 (2002) 93.
[15] G.J. Jin, G.Z. Lu, Y.L. Guo, Y. Guo, J.S. Wang, X.H. Liu, Catal. Lett. 87 (2003) 249.
[16] A. Takahashi, N. Hamakawa, I. Nakamura, T. Fujitani, Appl. Catal. A 294 (2005) 34.
[17] J. Lu, J.J. Bravo-Suárez, A. Takahashi, M. Haruta, S.T. Oyama, J. Catal. 232 (2005) 85.
[18] J. Lu, J.J. Bravo-Suárez, M. Haruta, S.T. Oyama, Appl. Catal. A 302 (2006) 283.
[19] W. Yao, Y. Guo, X. Liu, Y. Guo, Y. Wang, Y. Wang, Z. Zhang, G. Lu, Catal. Lett. 119 (2007) 185.
[20] Y. Lei, F. Mehmood, S. Lee, J. Greeley, B. Lee, S. Seifert, R.E. Winans, J.W. Elam, R.J. Meyer, P.C. Redfern, D. Teschner, R. Schlögl, M.J. Pellin, L.A. Curtiss, S. Vajda, Science 328 (2010) 224.
[21] M. Ojeda, E. Iglesia, Chem. Commun. (2009) 352.
[22] S. Lee, L.M. Molina, M.J. López, J.A. Alonso, B. Hammer, B. Lee, S. Seifert, R.E. Winans, J.W. Elanm, M.J. Pellin, S. Vajda, Angew. Chem. Int. Ed. 48 (2009) 1467.
[23] J. Huang, T. Akita, J. Faye, T. Fujitani, T. Takei, M. Haruta, Angew. Chem. Int. Ed. 48 (2009) 7862.
[24] R.L. Cropley, F.J. Williams, O.P.H. Vaughan, A.J. Urquhart, M.S. Tikhov, R.M. Lambert, Surf. Sci. 578 (2005) L85.
[25] R.L. Cropley, F.J. Williams, A.J. Urquhart, O.P.H. Vaughan, M.S. Tikhov, R.M. Lambert, J. Am. Chem. Soc. 127 (2005) 6069.
[26] D. Torres, N. Lopez, F. Illas, R.M. Lambert, Angew. Chem. Int. Ed. 46 (2007) 2055.
[27] J.R. Monnier, G.W. Hartley, J. Catal. 203 (2001) 253.
[28] J. Lu, M. Luo, H. Lei, X. Bao, C. Li, J. Catal. 211 (2002) 552.
[29] J. Lu, M. Luo, C. Li, Chin. J. Catal. 25 (2004) 5.
[30] O.P.H. Vaughan, G. Kyriakou, N. Macleod, M. Tikhov, R.M. Lambert, J. Catal. 236 (2005) 401.
[31] H. Chu, L. Yang, Q. Zhang, Y. Wang, J. Catal. 241 (2006) 225.
[32] Y. Wang, H. Chu, W. Zhu, Q. Zhang, Catal. Today 131 (2007) 495.
[33] W. Zhu, Q. Zhang, Y. Wang, J. Phys. Chem. C 112 (2008) 7734.
[34] W. Su, S. Wang, P. Ying, Z. Feng, C. Li, J. Catal. 268 (2009) 165.
[35] I. Onal, D. Düzenli, A. Seubsai, M. Kahn, E. Seker, S. Senkan, Top. Catal. 53 (2010) 92.
[36] S. Sato, R. Takahashi, T. Sodesawa, K. Yuma, Y. Obata, J. Catal. 196 (2000) 195.
[37] A. Gervasini, S. Bennici, Appl. Catal. A 281 (2005) 199.
[38] J. Morales, J.P. Espinos, A. Caballero, A.R. Gonzalez-Elipe, J.A. Mejias, J. Phy. Chem. B 109 (2005) 7758.
[39] G. Silversmit, D. Depla, H. Poelman, G.B. Marin, R.D. Gryse, J. Electron Spectrosc. Relat. Phenom. 135 (2004) 167.
[40] J.L. Callahan, R.K. Grasselli, AIChE J. 9 (1963) 755.
[41] B.J. Wood, H. Wise, R.S. Yolles, J. Catal. 15 (1969) 355.
[42] T. Inui, T. Ueda, M. Suehiro, J. Catal. 65 (1980) 166.